US009403275B2

(12) **United States Patent**
Hoffmann et al.

(10) **Patent No.: US 9,403,275 B2**
(45) **Date of Patent: Aug. 2, 2016**

(54) **DYNAMIC OBSTACLE AVOIDANCE IN A ROBOTIC SYSTEM**

(71) Applicant: **GM GLOBAL TECHNOLOGY OPERATIONS LLC**, Detroit, MI (US)

(72) Inventors: **Heiko Hoffmann**, Simi Valley, CA (US); **Derek Mitchell**, Calabasas, CA (US)

(73) Assignee: **GM Global Technology Operations LLC**, Detroit, MI (US)

(*) Notice: Subject to any disclaimer, the term of this patent is extended or adjusted under 35 U.S.C. 154(b) by 18 days.

(21) Appl. No.: **14/517,245**

(22) Filed: **Oct. 17, 2014**

(65) **Prior Publication Data**

US 2016/0107313 A1 Apr. 21, 2016

(51) **Int. Cl.**
B25J 9/16 (2006.01)

(52) **U.S. Cl.**
CPC ***B25J 9/1666*** (2013.01); ***B25J 9/1697*** (2013.01); *G05B 2219/40475* (2013.01); *G05B 2219/40476* (2013.01); *G05B 2219/40519* (2013.01)

(58) **Field of Classification Search**
CPC B25J 9/1666; B25J 9/1697; G05B 2219/40475; G05B 2219/40476; G05B 2219/40519
See application file for complete search history.

(56) **References Cited**

U.S. PATENT DOCUMENTS

6,054,997	A	4/2000	Mirtich	
8,160,744	B2	4/2012	Nagasaka et al.	
2003/0225479	A1*	12/2003	Waled	B25J 9/161 700/245
2004/0073414	A1*	4/2004	Bienenstock	G06F 3/015 703/2
2005/0126833	A1*	6/2005	Takenaka	B25J 13/088 180/8.1
2009/0105878	A1*	4/2009	Nagasaka	B25J 13/084 700/245
2009/0259337	A1*	10/2009	Harrold	B25J 9/1692 700/245
2010/0168950	A1*	7/2010	Nagano	B25J 9/1666 701/25
2012/0180983	A1*	7/2012	Ishikawa	G03B 27/32 165/61
2012/0320361	A1*	12/2012	Ishikawa	G03B 27/32 355/72
2013/0138244	A1*	5/2013	Nagasaka	B25J 9/1612 700/245
2013/0158840	A1*	6/2013	Lu	F02D 41/2432 701/104

(Continued)

FOREIGN PATENT DOCUMENTS

DE	102009006256	A1	7/2010
EP	1901150	A1	3/2008
EP	1901151	A1	3/2008

OTHER PUBLICATIONS

S. Mohammmad Khansari-Zadeh and Aude Billard; "Realtime Avoidance of Fast Moving Objects: A Dynamical System-Based Approach"; Ecole Polytechnique Federale de Lausanne, LASA Laboratory.

(Continued)

Primary Examiner — Rodney Butler
(74) *Attorney, Agent, or Firm* — Quinn Law Group, PLLC

(57) **ABSTRACT**

A robotic system includes an end-effector, an input device, and a controller. The input device is operable for collecting data defining a position and a velocity of a dynamic obstacle in an environment of the end-effector. The dynamic obstacle has an arbitrary shape. The controller is in communication with the end-effector and is programmed to execute a method and thereby receive a set of inputs via the input device, including the position and velocity of the dynamic obstacle. The controller computes a contour function defining the closest allowed distance and direction between the end-effector and the dynamic obstacle using the Gilbert-Johnson-Keerthi algorithm, and controls the end-effector via an output command to thereby avoid contact between the end-effector and the dynamic obstacle.

8 Claims, 3 Drawing Sheets

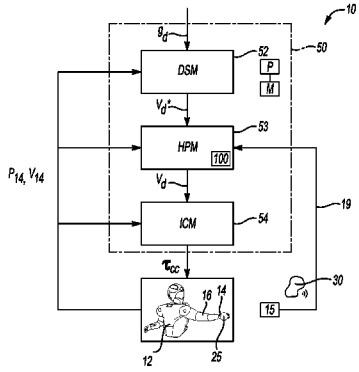

(56) **References Cited**

U.S. PATENT DOCUMENTS

2013/0226344	A1*	8/2013	Wong	G05D 1/024 700/258
2013/0331644	A1*	12/2013	Pandya	A61B 19/2203 600/102
2013/0345875	A1*	12/2013	Brooks	B25J 9/0087 700/259
2015/0010202	A1*	1/2015	Tuzel	G06T 7/0046 382/103
2015/0066199	A1*	3/2015	Shimono	B65G 59/04 700/218

OTHER PUBLICATIONS

S.M. Khansari-Zadeh and Aude Billard; "A Dynamical System Approach to Realtime Obstacle Avoidance"; Ecole Polytechnique Federale de Lausanne, LASA Laboratory.

Patrick Lindemann: "The Gilbert-Johnson-Keerthi Distance Algorithm"; Media Informatics Proseminar on "Algorithms in Media Informatics", 2009.

Heiko Hoffmann, Peter Pastor, Dae-Hyung Park, Stefanschaal; "Biologically-inspired dynamical systems for movement generation: automatic real-time goal adaptation and obstacle avoidance".

* cited by examiner

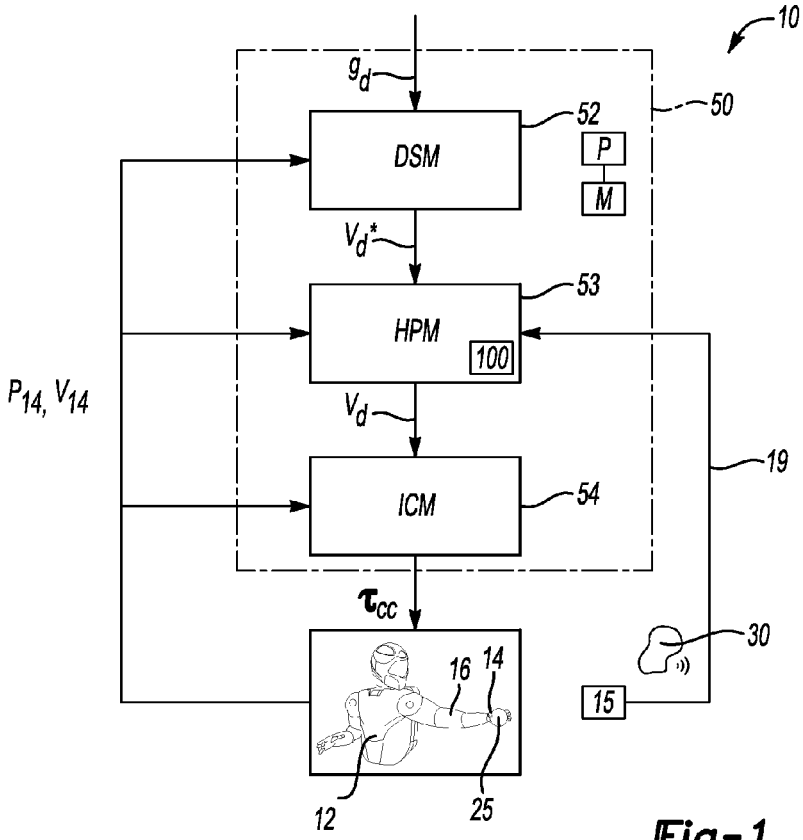
10
g_d
50
52
DSM
P
M
V_d*
53
HPM
100
P_{14}, V_{14}
V_d
19
ICM
54
τ_{cc}
30
16
14
15
12
25

Fig-1

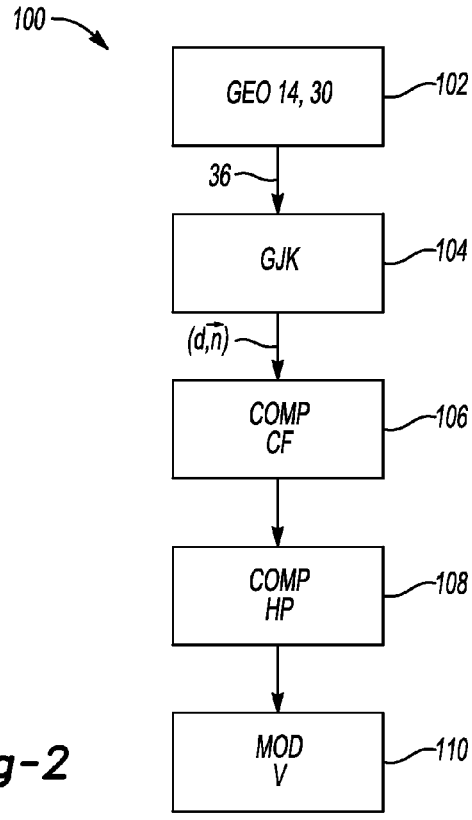
100
GEO 14, 30
102
36
GJK
104
$(\hat{d},\bar{n})$
COMP CF
106
COMP HP
108
MOD V
110

Fig-2

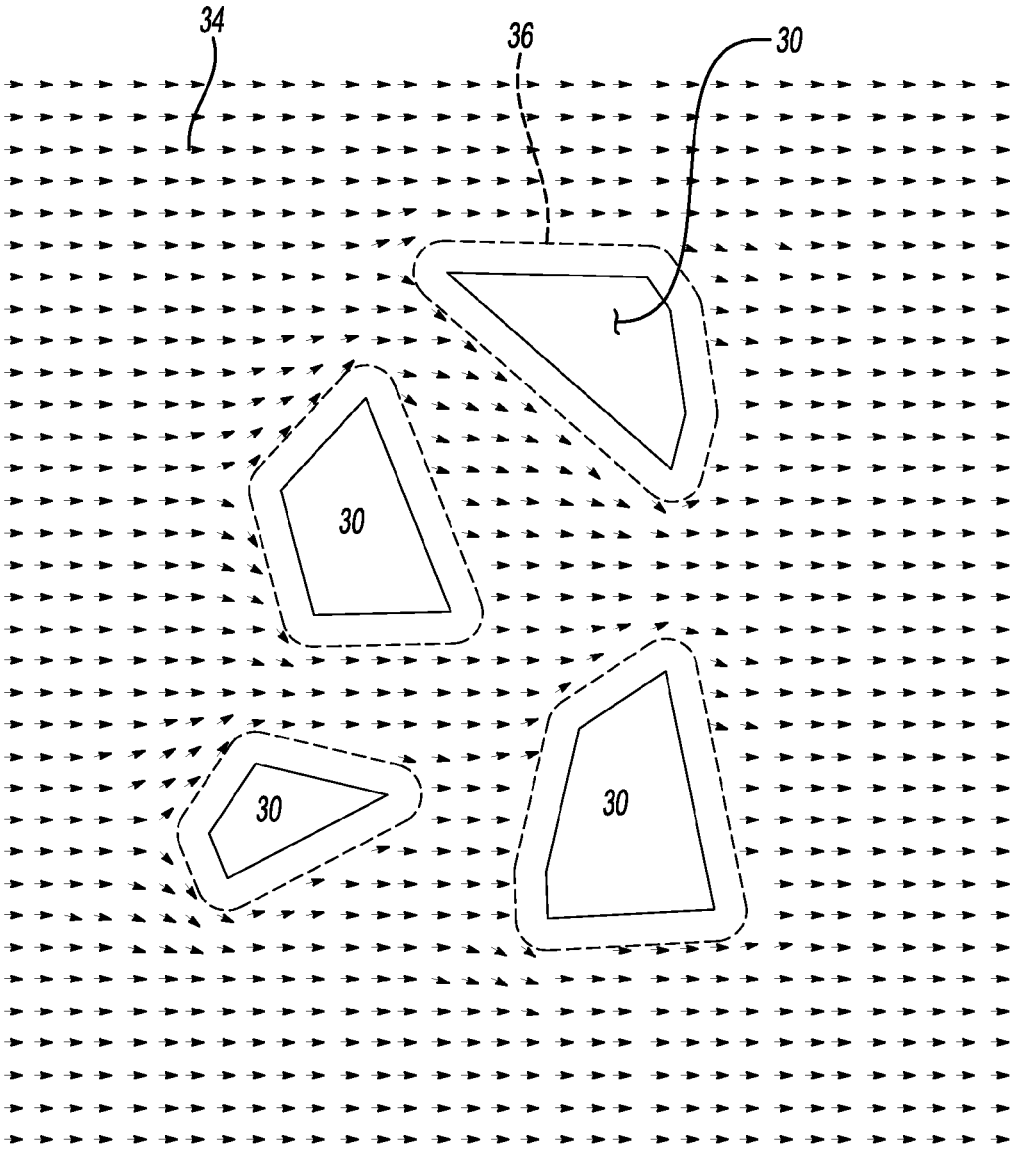

Fig-3A

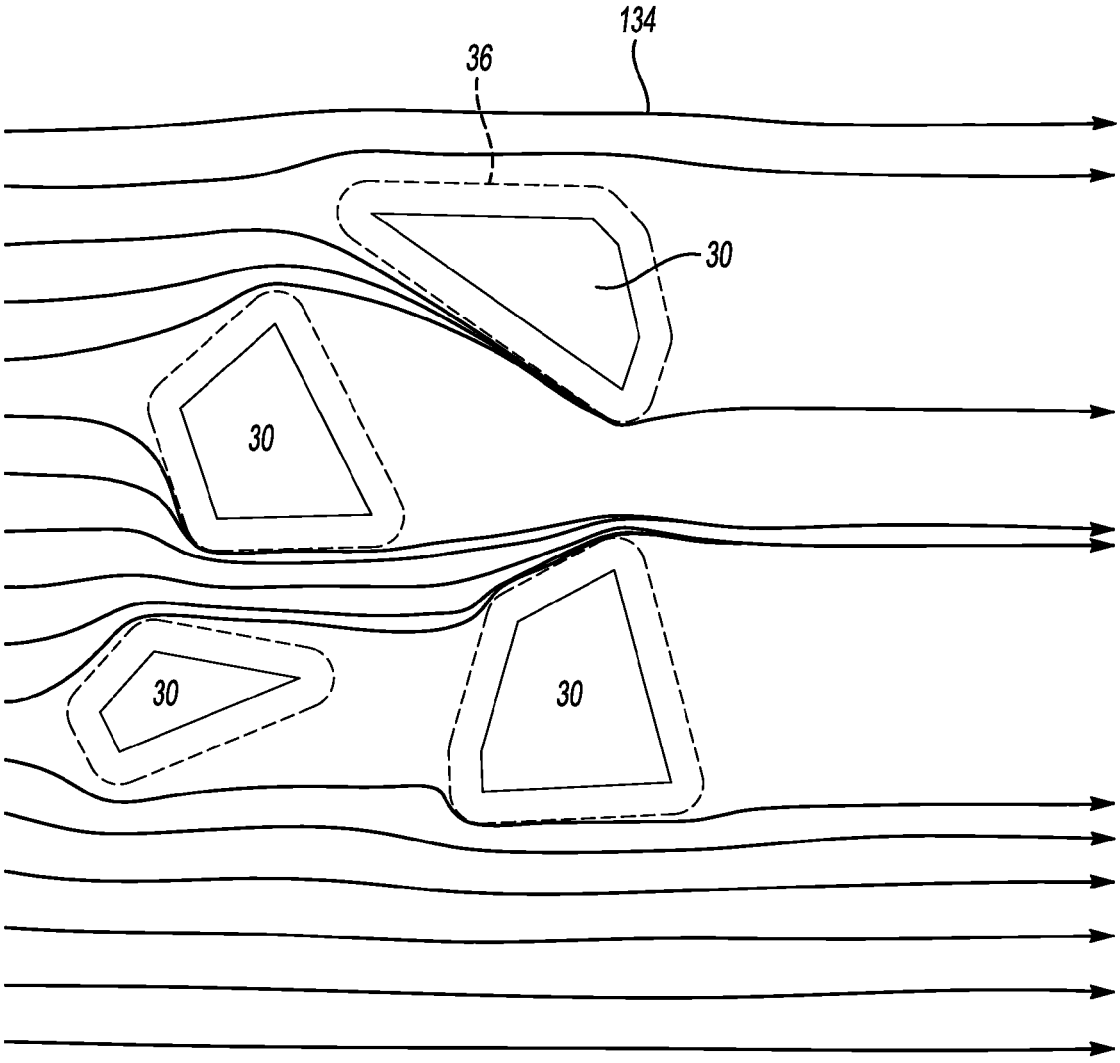

Fig-3B

DYNAMIC OBSTACLE AVOIDANCE IN A ROBOTIC SYSTEM

TECHNICAL FIELD

The present disclosure relates to dynamic obstacle avoidance in a robotic system.

BACKGROUND

Robots typically include a series of linkages that are interconnected via motor-driven robotic joints. Each robotic joint represents one or more independent control variables or degrees of freedom. End-effectors such as robotic hands, grippers, and the like are the particular end linkages which act on an object in the performance of a commanded work task, for instance the grasping and moving of an object. Complex programming and motion control logic is used in a variety of ways to achieve the required levels of robotic mobility, dexterity, and work task-related functionality. End-effectors typically approach and depart from a specified goal position according to a defined path or trajectory. Such paths are pre-planned using a variety of techniques. However, conventional end-effector path planning techniques may be less than optimally robust when encountering dynamic obstacles in the work environment.

SUMMARY

A robotic controller is described herein that is suitable for controlling an end-effector in the presence of dynamic obstacles. Unlike existing approaches, the controller uses the Gilbert-Johnson-Keerthi (GJK) algorithm to compute a contour function and thereby allow the controller to deal with dynamic obstacles having an arbitrary shape, i.e., not predefined. The present methodology also uses harmonic potentials to modulate a motion plan for the end-effector, thereby steering the end-effector around such dynamic obstacles in the robot's work environment.

Specifically, the controller considers the velocity of the dynamic obstacle as an input and computes a distance between arbitrary geometric shapes representing the obstacles. This approach utilizes the GJK algorithm to compute the distance. Thus, a contour function is defined by the controller for avoiding encountered dynamic obstacles, as opposed to using predefined contour functions and defined/non-arbitrary obstacle shapes. This approach also allows the controller to use the capabilities of point cloud shapes, and for a given control point to be represented as a volume with a defined shape. In this manner, the concept of harmonic potentials is extended to situations in which the dynamic obstacles are presented as a collection of points, for instance from a 3D point cloud camera that outputs point clouds or Light Detection and Ranging (LIDAR) scans of the obstacles. Additionally, the present design contemplates automatic adjustment of a modulation function so that obstacle velocities are considered, thereby allowing the controller to better avoid the dynamic obstacles.

The above and other features and advantages of the present disclosure are readily apparent from the following detailed description when taken in connection with the accompanying drawings.

BRIEF DESCRIPTION OF THE DRAWINGS

FIG. **1** is a schematic illustration of an example robotic system having a robot and a controller that combines a dynamical system utilizing flow fields with harmonic potentials for the purpose of avoiding arbitrarily-shaped dynamic obstacles.

FIG. **2** is a schematic logic flow diagram describing an example harmonic potential modulator approach usable within the robotic system of FIG. **1**.

FIG. **3**A is a schematic vector field.

FIG. **3**B is a schematic streamlined variant of the vector field shown in FIG. **3**A.

DETAILED DESCRIPTION

With reference to the drawings, wherein like reference numbers refer to the same or similar components throughout the several views, a robotic system **10** is shown schematically in FIG. **1** having a controller **50**. The robotic system **10** includes a robot **12**. The robot **12** is depicted as an example dexterous humanoid robot in FIG. **1**, but the robot **12** may be alternatively embodied as any multi-axis robot. The robot **12** operates in the presence of dynamic obstacles **30**, e.g., moving operators, other robots, and the like. The controller **50** is programmed to avoid the dynamic obstacles **30** via execution of a method **100**, with an example embodiment of the method **100** shown in FIG. **2**. Example dynamic obstacles **30** and associated flow fields are shown schematically in FIGS. **3**A and **3**B.

The robot **12** includes an end-effector **14** such as a gripper or a multi-fingered hand disposed at a distal end of a robot arm **16**. Motion of the robot **12**, particularly of the end-effector **14** and the robot arm **16**, is automatically controlled via a robotic controller **50** having a dynamical system module (DSM) **52**, a harmonic potential modulator (HPM) **53**, and an impedance control module (ICM) **54**, the specific programmed functions of which are described in detail below. A camera **15** such as a 3D point cloud camera, a LIDAR sensor array, or the like collects a set of 3D point cloud information describing the location and approximate geometry of the dynamic obstacles **30** and relays this information to the controller **50** as point cloud data (arrow **19**) as part of the method **100**.

The robot **12** is programmed in software and equipped in hardware to perform one or more automated tasks with multiple control degrees of freedom, such as grasping and moving an object **25** with a changing position and velocity, and to perform other interactive tasks or control other integrated system components, for instance clamping, relays, task lighting, and the like. In the embodiment shown in FIG. **1**, the robot **12** includes a plurality of independently and interdependently-moveable robotic joints to control motion of the robot arm **16** and the end-effector **14**. Although omitted from FIG. **1** for illustrative simplicity, each robotic joint contains and/or is driven by one or more joint actuators, such as a joint motor, linear actuator, rotary actuator, or the like.

The controller **50** of FIG. **1** provides precise motion control of the robot **12**, including control over the fine and gross movements needed for manipulating an object (not shown) that may be acted on by the end-effector **14**. Additionally, the controller **50** provides online movement generation and motor control for the robot **12**. The DSM **52** can be programmed to provide a dynamic movement primitive (DMP) as known in the art, thus generating a motion trajectory in real time using differential equations.

In particular, the controller **50** is intended to improve upon existing approaches toward avoidance of obstacles, e.g., the example moving/dynamic obstacles **30** shown in FIG. **1**. Specifically, the controller **50** utilizes the HPM **53** to modulate motion of the end-effector **14** and thereby steer the end-effector **14** around the dynamic obstacles **30**, such as is shown

schematically via the streamlines **134** of FIG. **3**B. Harmonic potentials as applied in the art of robotic control are valued for having capabilities similar to potential field avoidance, but without requiring the treatment of local minima. For example, some conventional approaches define continuous contour functions for each static obstacle in order to modulate control point velocities in the vicinity of such an obstacle.

The controller **50** of FIG. **1** as configured herein utilizes the Gilbert-Johnson-Keerthi (GJK) algorithm to define a contour function, as opposed to prior art approaches which deal with obstacles of defined shape via predefined contour functions. The GJK algorithm is ultimately used by the controller **50** to shape a flow field for control of the end-effector **14** as explained below. This function provides the capability of using point cloud shapes from the camera **15** as well as allowing any particular control point to be represented as a volume with a defined shape. In this way, harmonic potential methods can be readily extended to handle situations in which the dynamic obstacles **30** of FIGS. **1**, **3**A, and **3**B are presented as a collection of points collected by the camera **15**.

Additionally, the controller **50** of FIG. **1** is programmed to adjust a modulation function via the HPM **53** in such a way as to consider the velocities of the dynamic obstacles **30** in proximity to the robot **12**. This approach allows the controller **50** to better avoid the dynamic obstacles **30**, even if the obstacles **30** are moving at a significant speed and the control volume has no inherent velocity.

The controller **50** may be structurally embodied as a computer device or multiple such devices programmed to plan and generate robotic movements of the robot arm **16** and the end-effector **14**. The control system **50** may include one or more processors (P) and memory (M), including sufficient amounts of tangible, non-transitory memory. Memory types may include optical or magnetic read only memory (ROM), random access memory (RAM), erasable electrically-programmable read only memory (EEPROM), and the like. The control system **50** may also include a high-speed clock, analog-to-digital (A/D) circuitry, digital-to-analog (D/A) circuitry, and any required input/output (I/O) circuitry and devices, as well as signal conditioning and buffer electronics. Individual control algorithms resident in the controller **50** or readily accessible thereby, such as instructions embodying the method **100** of FIG. **2**, may be stored in memory (M) and automatically executed via the processor (P) at one or more different control levels to provide the respective control functionality.

A dynamic movement primitive (DMP), as is well known in the art of robotic control, can be used to generate a particular robotic movement trajectory x(t) with a given velocity v(t). The equations of motion for a DMP are motivated by the dynamics of a damped spring attached to a goal position g and perturbed by a non-linear acceleration:

$$\dot{v}=K(g-x)-Dv+(g-x_0)f(s)$$

$$\dot{x}=v$$

where x_0 is the start point of a given movement, K is the spring constant, D is the damping constant, and f is a parameterized non-linear function.

In general, the controller **50** shown schematically in FIG. **1** receives a similar desired goal (g_d), i.e., a defined target position of a given movement of the end-effector **14**, either via programming or via a specified reference path provided via demonstration learning, and executes such a set of differential equations via the DSM **52**. The DSM **52** outputs a desired joint velocity (v_d*) to and interacts with the HPM **53**, which ultimately transmits a modified joint velocity (v_d) to the ICM **54**. The ICM **54** in turn calculates and transmits a commanded motor torque command (τ_{CC}) to the robot **12** via an impedance framework, as is well known in the art, and along with the HPM **53** receives or determines an actual joint position (P_{14}) and an actual velocity (V_{14}) from the robot **12**. As is known in the art, the position may be measured via a position sensor (not shown) and the actual velocity may be calculated by the controller **50** from a series of such measured joint positions over time.

FIG. **2** describes an example general embodiment of the method **100**. Further details of the various steps are provided below. At step **102**, the controller **50** of FIG. **1** uploads the positions and geometry (GEO) of the end-effector **14** and the dynamic obstacles **30**. The dynamic obstacles **30** may be detected, as noted above, as a point cloud using the camera **15**, i.e., by processing the point cloud data (arrow **19**) streamed from the camera **15** to the controller **50**. As part of the method **100**, the controller **50** extends the concept of harmonic potential avoidance so that it can be applied to the dynamic obstacles **30**, with each dynamic obstacle having an arbitrary shape.

Referring briefly to FIGS. **3**A and **3**B, the dynamic obstacles **30** are depicted as arbitrarily-shaped polygons. In FIG. **3**A, the dynamic obstacles **30** are initially located in a flow field **34** of a constant flow, with the flow field **34** representing as vectors all the possible motion of the end-effector **14** with respect to the dynamic obstacles **30**. FIG. **3**B depicts streamlines **134** of a modulated version of the flow field **34** shown in FIG. **3**A after execution of the method **100**. The controller **50** forms an artificial boundary **36** around the dynamic obstacles **30** for avoidance of the dynamic obstacles **30** as part of the method **100** as explained below.

Referring again to FIG. **2**, the output of step **102** is the shape of the boundary **36** shown in FIGS. **3**A and **3**B. Using the shape of the boundary **36**, the controller **50** next executes the GJK algorithm at step **104** in real time while the robot **12** moves, and to compute the distance (d) and direction ($\vec{n}$) between the end-effector **14** and the dynamic obstacles **30**. With S representing the shape of the boundary **36**, the controller **50** determines the distance (d) and direction ($\vec{n}$) between the robot arm **16** or end-effector **14** and the obstacle **30**:

$$(d,\vec{n})=GJK(S_{control},S_{obstacle})$$

In the above equation $S_{control}$ is the predefined or known shape of the end-effector **14** and/or arm **16** of FIG. **1**, e.g., a polygon convex hull around the end-effector **14**, and $S_{obstacle}$ is the shape of the obstacle **30**. The output of GJK algorithm, particularly the distance (d), is fed into step **106**.

At step **106** the controller **50** defines a contour function, $\Gamma_k(\xi_k)$, using the result of step **104**. The contour function is ultimately stated as $\Gamma(d)=(m(d-\eta)+1)^{\rho}$. The contour function is represented as CF in step **106** of FIG. **2** for illustrative clarity. The above parameters affect the strength of any repulsive force around the obstacle **30**, with m defining the scale of the distance metric, i.e., effectively regulating how quickly the contour function $\Gamma_k(\xi_k)$ increases as a function of distance (d), η represents a safety envelope which defines the distance from a given obstacle **30** at which the velocity normal to the surface of the obstacle **30** is zero, and ρ is the reactivity of the potential field around the obstacle **30**, which also affects how quickly the contour function $\Gamma_k(\xi_k)$ increases with distance (d).

From this, the controller **50** of FIG. **1** next computes the harmonic potential at step **108**, i.e.,

$$\sum_{k=1}^{N} M_k(\xi_k)\dot{\xi}_k.$$

The velocity of the end-effector **14** is then modulated via the DSM **52** using the dynamical system, with f(t,ξ) being the velocity output from the dynamical system function of the DSM **52**, i.e., V_d* as shown in FIG. **1**.

Harmonic potentials are used by the controller **50** at step **110** to modify the control velocity V_d* derived in the vicinity of the dynamic obstacles **30** via the DSM **52**. In conventional approaches, this modification is performed for a single obstacle **30** by representing the modulation as a matrix and considering the factorized form:

$$M(\xi)=E(\xi)D(\xi)E(\xi)^{-1}$$

$$\dot{\xi}=M(\xi)f(t,\xi)$$

where D is a diagonal matrix of eigenvalues of the following form:

$$D(\xi)=\begin{bmatrix}\lambda^1(\xi) & & 0\\ & \ddots & \\ 0 & & \lambda^d(\xi)\end{bmatrix}$$

$$\lambda^i(\xi)=\begin{cases}1-\dfrac{1}{|\Gamma(\xi)|} & i=1\\ 1+\dfrac{1}{|\Gamma(\xi)|} & 2\le i\le d\end{cases}$$

and E is a set of basis vectors of the form:

$$E(\xi)=\begin{bmatrix}\dfrac{\partial\Gamma(\xi)}{\partial\xi_1} & -\dfrac{\partial\Gamma(\xi)}{\partial\xi_2} & \cdots & \dfrac{d\Gamma(\xi)}{\partial\xi_d}\\ \vdots & \dfrac{\partial\Gamma(\xi)}{\partial\xi_1} & & 0\\ & & \ddots & \\ \dfrac{\partial\Gamma(\xi)}{\partial\xi_d} & 0 & & \dfrac{\partial\Gamma(\xi)}{\partial\xi_1}\end{bmatrix}$$

For the above equations, ξ represents a state variable of the distance dimension d, Γ is a scalar function that equals 1 at the contour of a shape and increases monotonically with increasing distance from the shape,

$$\frac{\partial\Gamma(\xi)}{\partial\xi_i}$$

denotes the gradient of Γ(ξ) along the i^{th} dimension, and f(t,ξ), once again, is the velocity output from the DSM **52**, i.e., V_d*. This velocity expression may be replaced by another control velocity to apply harmonic potential avoidance to other forms of control.

The above approach is then modified by the controller **50** to consider velocities of multiple dynamic obstacles **30**. For multiple dynamic obstacles **30**, the modulation matrix (M) noted above is evaluated via the controller **50** in the frame of reference of each dynamic obstacle **30** of FIG. **1** and then combined as a weighted product. The modification may be performed by adjusting the eigenvalues so that the global modulation matrix (M) is represented as the sum of individual components rather than as a product as in the above expressions. This approximation loses the coupling terms created by multiplying the modulation matrices of different obstacles **30** together. The coupling terms define the potential in the area between two obstacles **30** in close proximity to each other, but their contributions are small and thus can be ignored. The result of the above modification is represented mathematically as follows:

$$M_k(\xi_k)=E_k(\xi_k)D_k(\xi_k)E_k(\xi_k)^{-1}$$

$$D_k(\xi_k)=\begin{bmatrix}\lambda_k^1(\xi) & & 0\\ & \ddots & \\ 0 & & \lambda_k^d(\xi)\end{bmatrix}$$

$$\lambda_k^i(\xi_k)=\begin{cases}-\dfrac{\omega_k(\xi_k)}{|\Gamma_k(\xi_k)|} & i=1\\ \dfrac{\omega_k(\xi_k)}{|\Gamma_k(\xi_k)|} & 2\le i\le d\end{cases}$$

Here, the weights ω_k are defined by evaluating the contour function $\Gamma_k(\xi_k)$ for each dynamic obstacle **30**:

$$\omega_k(\xi_k)=\prod_{i=1,i\neq k}^{N}\frac{\Gamma_i(\xi_i)-1}{\Gamma k(\xi_k)-1+\Gamma_i(\xi_i)-1}$$

$$\dot{\xi}=f(t,\xi)+\sum_{k=1}^{N}M_k(\xi_k)\dot{\xi}_k$$

$$\dot{\xi}=f(t,\xi)-v_k$$

This allows the controller **50** of FIG. **1** to evaluate the velocity of the dynamic obstacles **30** in each frame of reference of the dynamic obstacles **30** before combining the weighted contributions in the global frame of reference.

To make proper use of the method **100** of FIG. **2**, the controller **50** defines the contour function $\Gamma_k(\xi_k)$ and its gradient for each dynamic obstacle **30**. For basic shapes, the contour function and the gradient are trivial. For instance, a sphere with radius α would be represented as:

$$\Gamma(\xi)=\sum_{i=1}^{3}\left(\frac{\xi_i}{a}\right)^2$$

$$\frac{\partial\Gamma(\xi)}{\partial\xi_i}=2\frac{\xi_i}{a^2}$$

The contour function in this instance increases monotonically as a function of ξ and defines the contour of the circle when Γ(ξ)=1.

For more complex shapes, however, the contour function $\Gamma_k(\xi_k)$ leverages the GJK algorithm, as noted above in reference to step **104** of FIG. **2**, to define the closest distance (d) and direction ($\vec{n}$) between two shapes:

$$(d,\vec{n})=GJK(S_{control},S_{obstacle})$$

This equation arises from the standard application of the GJK algorithm, as known in the art. The inputs are the shape representations that define the control volume and the particular dynamic obstacle **30** in question. The outputs d and $\vec{n}$ represent the respective closest distance and the direction vector between the two point clouds describing two obstacles **30**. These outputs can be directly entered into the contour function and its gradient at step **106**:

$$\Gamma(d)=(m(d-\eta)+1)^{\rho} \quad \nabla\Gamma(d)=\rho m((m(d-\eta)+1)^{\rho-1})\vec{n}$$

The contour function should not encounter distance values of less than η. At Γ(d)=1, the harmonic avoidance acts to prevent the contour function from decreasing any further. It is possible that discrete time steps may cause the control volume to penetrate this boundary, but the potential field is still viable while Γ(d)>0. At this stage the control volume is guided outward until it reaches the obstacle surface, so the contour function should never reach zero or negative values.

A benefit of the present approach is that it extends to all forms of convex shapes. The GJK algorithm applied at steps **104** and **106** requires only that a support function be defined for the type of shape that is used. The term "support function" in this case refers to the function which defines the farthest point along a given direction. For a sphere, it is simply the radius projected onto the given direction. For a point cloud, it is the furthest point along that direction. As long as these functions are provided, the present approach can extend to any shape. If a concave shape is given, usage of the support function will ensure that only the convex hull is considered.

While the best modes for carrying out the present disclosure have been described in detail, those familiar with the art to which this disclosure relates will recognize various alternative designs and embodiments within the scope of the appended claims.

The invention claimed is:

1. A robotic system comprising:

an end-effector;

an input device operable for collecting data defining a position and a velocity of a dynamic obstacle in an environment of the end-effector, wherein the dynamic obstacle has an arbitrary shape; and

a controller in communication with the end-effector, wherein the controller is programmed to receive a set of inputs via the input device, including the position and velocity of the dynamic obstacle, to compute a contour function defining the closest allowed distance and direction between the end-effector and the dynamic obstacle using the Gilbert-Johnson-Keerthi (GJK) algorithm, and to control the end-effector via an output command to thereby avoid contact between the end-effector and the dynamic obstacle;

wherein the controller is programmed with a dynamical system module (DSM) which outputs a desired control velocity command to the end-effector as a commanded motion trajectory, and the set of inputs further includes an actual position and velocity of the end-effector and a desired goal position of the end-effector, and wherein the controller further includes a harmonic potential modulator (HPM) in communication with the DSM that receives the actual velocity of the end-effector, the position and velocity of the dynamic obstacle, and the desired control velocity command as inputs, and generates a modulated desired velocity command as part of the output command.

2. The robotic system of claim **1**, wherein the input device is a 3D point cloud camera and the data is 3D point cloud data.

3. The robotic system of claim **1**, wherein the input device is a LIDAR camera and the data is LIDAR data.

4. The robotic system of claim **1**, wherein the controller further includes an impedance control module (ICM) in communication with the HPM, wherein the ICM is programmed to receive the modulated desired velocity from the HPM and output a torque command as part of the output command to the end-effector to avoid the contact.

5. A method for avoiding contact between an end-effector of a robotic system and a dynamic obstacle in an environment, the method comprising:

collecting, via an input device, data defining a position and a velocity of a dynamic obstacle in the environment of the end-effector, wherein the dynamic obstacle has an arbitrary shape; and

receiving, via a controller, a set of inputs from the input device, including the position and a velocity of the dynamic obstacle;

computing a contour function defining the closest allowed distance and direction between the end-effector and the dynamic obstacle using the Gilbert-Johnson-Keerthi (GJK) algorithm;

using a dynamical system module (DSM) of the controller to output a desired control velocity command to the end-effector as a commanded motion trajectory, wherein the set of inputs further includes an actual position and velocity of the end-effector and a desired goal position of the end-effector, and wherein the controller further includes a harmonic potential modulator (HPM) in communication with the DSM;

receiving the actual velocity of the end-effector, the position and velocity of the dynamic obstacle, and the desired control velocity command via the HPM;

generating a modulated desired velocity command via the HPM; and

controlling the end-effector via an output command from the controller, including the modulated desired velocity command, to thereby avoid contact between the end-effector and the dynamic obstacle.

6. The method of claim **5**, wherein collecting data includes collecting a 3D point cloud camera via a 3D point cloud camera.

7. The method of claim **5**, wherein collecting data includes collecting LIDAR data via a LIDAR camera.

8. The method of claim **5**, wherein the controller further includes an impedance control module (ICM) in communication with the HPM, the method further comprising:

receiving, via the ICM, the modulated desired velocity from the HPM; and

outputting a torque command to the end-effector via the ICM as the output command to thereby avoid the contact.

* * * * *